Comparative neutron-shielding properties of metal oxide/HDPE composites using a Monte Carlo Code of PHITS

IOP Conf. Series: Materials Science and Engineering **526** (2019) 012013 doi:10.1088/1757-899X/526/1/012013

Comparative neutron-shielding properties of metal oxide/HDPE composites using a Monte Carlo Code of PHITS

W Poltabtim[1], D Toyen[1] and K Saenboonruang[1,2,*]

[1] Department of Applied Radiation and Isotopes, Faculty of Science, Kasetsart University, Bangkok 10900, Thailand
[2] Specialized center of Rubber and Polymer Materials in agriculture and industry (RPM), Faculty of Science, Kasetsart University, Bangkok, 10900, Thailand

* Corresponding author: kiadtisak.s@ku.th, fscikssa@ku.ac.th

Abstract. Development of efficient neutron-shielding materials has become one of the most important issues in radiation safety. In order to estimate shielding performances of the materials of interest, simulations of neutron-shielding characteristics using well-proved methods are necessary. In this work, a Monte Carlo code of Particle and Heavy Ion Transport code System (PHITS) was used to simulate neutron-shielding properties of HDPE composites that were added with either B_2O_3, Sm_2O_3, Gd_2O_3, or CdO as a filler at various contents. The energy of the incoming neutrons was fixed at 0.025 eV with the beam direction pointing at the right angle to the material's surface. The results showed that Gd_2O_3/HDPE composites had the lowest neutron transmission ratio compared with other fillers at the same contents, implying the highest neutron-shielding ability. Furthermore, the simulations also showed that the values of neutron transmission ratios of all fillers decreased with increasing filler's contents. Other information such as half-value-layer (HVL) and tenth-value-layer (TVL) were also simulated and reported in this work. We encouraged further investigation of this work by comparing the simulated results with the actual experiment in order to validate the accuracy of the simulation.

1. Introduction

Neutron technology has been utilized widely nowadays including water film thickness measurement [1], Boron Neutron-Capture Therapy (BNCT) [2], and analysis of ancient artifacts [3]. However, despite the benefits of neutron utilization, excessive exposure to neutrons could fatally harm users, ranging from skin burns, vomiting, dizziness, and possible death [4, 5].

To prevent and/or to reduce risks from radiation exposure, sufficient neutron shielding is required. In principle, good neutron shielding materials would compose of a combination of light elements such as hydrogen (H) or helium (He) and high-neutron-absorption-cross-section (σ_{abs}) elements such as boron-10 (^{10}B). Examples of such materials are B_2O_3/paraffin composites [6], B_2O_3/natural rubber (NR) [7], and nano-B_4C/high density polyethylene (HDPE) [8]. In particular, HDPE ($(C_2H_4)_n$) is one of common materials used in neutron shielding applications, mainly due to its high hydrogen content, which could effectively thermalize, i.e. reduce energy of, fast neutrons with higher efficiencies than other polymers such as NR or low density polyethylene (LDPE) [9]. HDPE also offers exceptional strength to density ratio and is able to withstand high temperatures (120°C).

In addition to light elements, high-σ_{abs} elements, especially ^{10}B, are also essential in thermal neutron attenuation. These elements could interact with incoming thermal neutrons, creating nuclear reactions and releasing other types of ionizing radiations such as alpha ($^4He^{2+}$) or proton ($^1H^+$) particles that are simpler to being shielded. One of the most commonly used elements having high σ_{abs} is boron, of which ^{11}B (80% abundance) has σ_{abs} of 0.0055 barns, while ^{10}B (20% abundance) has σ_{abs} of 3835 barns, making ^{10}B a better neutron absorber than a major isotope, ^{11}B. However, using purified ^{10}B as a neutron absorber would require complicated procedures to extract ^{10}B from natural boron (^{nat}B), hence, it would be much simpler and more cost effective to use ^{nat}B as a neutron absorber, although the resulting σ_{abs} would be reduced to 767 barns. The nuclear reactions between ^{10}B nuclei and thermal neutrons are shown in Eq. 1 and Eq. 2, in which 94% of all nuclear reactions would produce 0.48-MeV gamma (γ) rays.

$$^{10}B^{5+} + n \rightarrow {}^4He^{2+} + {}^7Li^{3+} \ (6\%) \quad (1)$$
$$^{10}B^{5+} + n \rightarrow {}^4He^{2+} + {}^7Li^{3+} + \gamma \ (94\%) \quad (2)$$

However, ^{nat}B is not the only element that could be used as a neutron absorber, other elements such as samarium (^{nat}Sm), gadolinium (^{nat}Gd), and cadmium (^{nat}Cd) that have σ_{abs} of 5,922 barns, 49,700 barns, and 2,520 barns, respectively, also have potentials to be used as effective neutron absorbers due to their high σ_{abs}. The neutron reactions between ^{149}Sm, ^{157}Gd, or ^{113}Cd nuclei (having the highest σ_{abs} among their respective isotopes) and thermal neutrons are shown in Eq. 3–5.

$$^{149}Sm^{62+} + n \rightarrow {}^4He^{2+} + {}^{146}Nd^{60+} \quad (3)$$
$$^{157}Gd^{64+} + n \rightarrow {}^{158}Gd^{64+} + \gamma \quad (4)$$
$$^{113}Cd^{48+} + n \rightarrow {}^{114}Cd^{48+} + \gamma \quad (5)$$

As seen by the high σ_{abs} of ^{nat}B, ^{nat}Sm, ^{nat}Gd, and ^{nat}Cd, this work aimed to simulate their thermal neutron shielding properties of their respective oxide compounds (B_2O_3, Sm_2O_3, Gd_2O_3, and CdO) in HDPE using a Monte Carlo code of Particle and Heavy Ion Transport code System (PHITS) [10, 11]. Important properties including neutron transmission ratio (I/I_0), half-value-layer (HVL), and tenth-value-layer (TVL), were thoroughly determined using the results from this simulation.

2. Experimental

PHITS is a multi-purpose Monte Carlo simulation package that could be used in various applications including the design of spacecraft and accelerator facilities. In this work, PHITS was used to simulate thermal neutron shielding properties of metal oxide/HDPE composites by considering their transport and collision processes. To set up the simulation, a thermal neutron beam (0.025 eV) with 0.1-mm diameter was pointed at a right angle to the surface of shielding materials (z axis). The sizes of all samples were 40 cm × 40 cm with their thicknesses varied from 0.2–1.0 cm in 0.2-cm increments and the detector with 100% detection efficiency was located at 20 cm away from the surface of the shielding materials. The setup of the simulation is shown in Fig.1. It should be noted that all simulations were performed in air conditions.

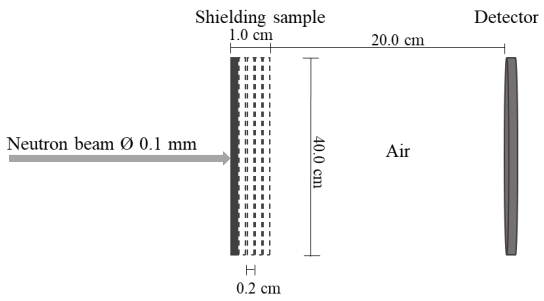

Fig. 1. Setup of the simulation to determine thermal neutron attenuation using PHITS.

Contents of all metal oxides in the HPDE composites used for the simulations were 10wt%, 20wt%, and 30wt%, respectively. The neutron attenuation could be calculated using Eq. 6;

$$I = I_0 e^{-\mu x} \quad (6)$$

where I, I_o, μ, and x are transmitted neutron intensity, initial neutron intensity, linear attenuation coefficient, and thickness of the sample. The values of HVL and TVL were determined using Eq. 7 and Eq. 8. It should be noted that μ used in the calculation of HVL and TVL was calculated using the results of the samples with 2-mm thickness due to the least effect from build-up factors [12].

$$HVL = \ln(2)/\mu \quad (7)$$
$$TVL = \ln(10)/\mu \quad (8)$$

3. Results and Discussion

As shown in Fig. 2, Gd_2O_3/HDPE composites could attenuate thermal neutrons with the highest efficiency as seen by the lowest numbers of transmitted neutrons. This was due to the fact that ^{nat}Gd nuclei have the highest value of σ_{abs}, leading to a larger probability of neutron interactions and absorption. Fig.3 illustrates effects of sample thicknesses to neutron shielding ability. The results showed that, as samples became thicker, less neutron could transmit. This was mainly due to higher numbers of metal oxides in thicker samples that could interact with neutrons, resulting in more neutron attenuation.

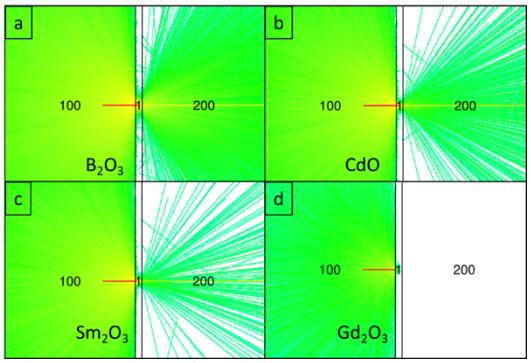

Fig.2. Results from PHITS simulation showing thermal neutron transmission of (a) B_2O_3/HDPE, (b) CdO/HDPE, (c) Sm_2O_3/HDPE, and (d) Gd_2O_3/HDPE composites. All samples were 10 mm thick with 30wt% metal oxide content.

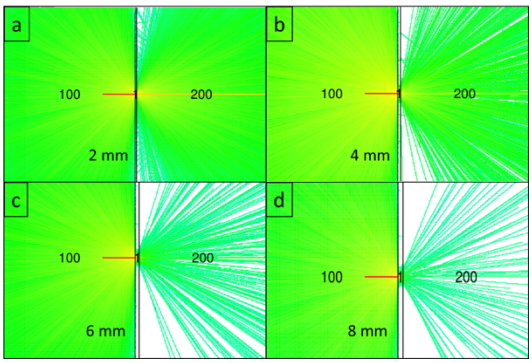

Fig.3. Results from PHITS simulation showing thermal neutron transmission of 10wt% Gd_2O_3/HDPE composites with (a) 2 mm, (b) 4 mm, (c) 6 mm, and (d) 8 mm thickness.

In terms of the values of neutron transmission ratios (I/I_0) shown in Fig. 4 and HVL/TVL values presented in table 1, it was obvious that Gd_2O_3/HDPE composites had the highest neutron shielding ability as illustrated by the lowest I/I_0, HVL, and TVL values compared with other composites. Another interesting result was that the ability to attenuate neutrons improved with increasing contents of metal oxide. This was because, as contents of metal oxide became larger, numbers of high-σ_{abs} nuclei that could effectively absorb thermal neutrons increased, leading to more interactions and less neutron transmission.

Table 1. Values of HVL and TVL of all HDPE composites.

Content (wt%)	Metal oxide							
	B_2O_3		Sm_2O_3		Gd_2O_3		CdO	
	HVL (cm)	TVL (cm)	HVL (cm)	TVL (cm)	HVL (cm)	TVL (cm)	HVL (cm)	TVL (cm)
10	6.23	20.71	3.30	10.97	0.44	1.47	3.24	10.76
20	2.66	8.84	1.62	5.41	0.23	0.78	1.73	5.75
30	1.73	5.77	1.11	3.70	0.17	0.58	1.27	4.23

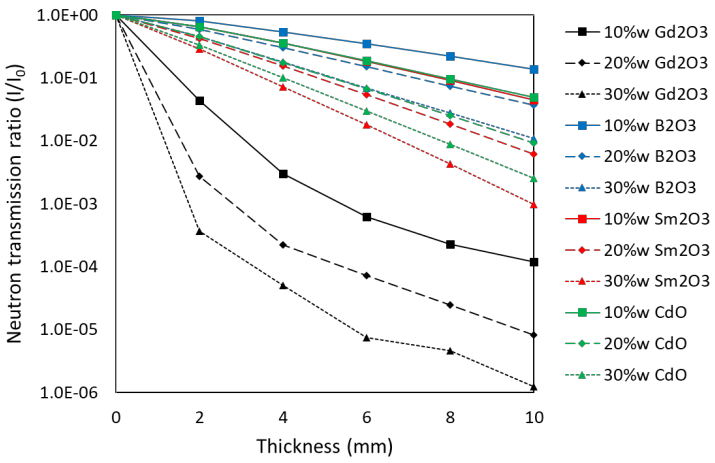

Fig.4. Neutron transmission ratios (I/I_0) of all HDPE composites. Note that the data are plotted in log scale.

4. Conclusions

PHITS was used to simulate thermal neutron shielding properties of HDPE composites that were added with either B_2O_3, Sm_2O_3, Gd_2O_3, or CdO as a neutron absorber. The results indicated that increasing metal oxide contents in HDPE composites led to the increases in thermal neutron shielding ability as seen by the decreases in neutron transmission ratios (I/I_0), HVL, and TVL. Furthermore, the results also showed that Gd_2O_3/HDPE composites had higher neutron shielding ability compared with other composites at the same contents.

5. References

[1] Dupont J, Mignot G, Zboray R and Prasser H M 2016 *J. Nucl. Sci. Technol.* **53** 673–81
[2] Chadha M, Capala J, Coderre J A, Elowitz E H, Iwai J, Joel D D, Lie H B, Wielopolski L and Chanana A D 1998 *Int. J. Radiat. Oncol. Biol. Phys.* **40** 829–34
[3] Boulanger M T, Buchanan B, O'Brien M J, Redmond B G, Glascock M D and Eren M I 2015 *J. Archaeol.* **53** 550–8
[4] Pinkerton L E, Waters M A, Hein M J, Zivkovich Z, Schubauer-Berigan M K and Grajewski B 2011 *Am. J. Ind. Med.* **55** 25–36
[5] El-Taher A and Uosif M A M 2006 *J. Phys. D: Appl. Phys.* **39** 20
[6] Toyen D and Saenboonruang K 2017 *J. Nucl. Sci. Techol.* **54** 871–7
[7] Ninyong K, Wimolmala E, Sombatsompop N and Saenboonruang K 2017 *Polym. Test.* **59** 336–43
[8] Kim J, Lee B C, Uhm Y R and Miller W 2014 *J. Nucl. Mater.* **453** 48–53
[9] Zuin L, Innocenti F, Fabris D, Lunardon M, Nebbia G, Viesti G, Cinausero M, Fioretto E, Prete G, Palomba M and Pantaleo A 2000 *Nucl. Instrum. Methods Phys. Res. A.* **449** 416–26
[10] Iwase H, Niita K and Nakamura T 2002 *J. Nucl. Sci. Techol.* **39** 1142–51
[11] Niita K, Sato T, Iwase H, Nose H, Nakashima H and Sihver L 2006 *Radiat. Meas.* **41** 1080–90
[12] Suteau C and Chiron M 2005 *Radiat. Prot. Dosimetry.* **116** 489–9

Acknowledgements

Authors would like to acknowledge technical supports from the Thailand Institute of Nuclear Technology (TINT) and Japan Atomic Energy Agency (JAEA). Authors also would like to thank the Specialized center of Rubber and Polymer Materials for agriculture and industry (RPM), Faculty of Science, Kasetsart University for the publication support.